Frequency-Responsive Refrigerator Switching Controller

Sumit Nema, *Student Member, IEEE,* Vivek Prakash, *SMIEEE,* Hrvoje Pandžić, *SMIEEE*

***Abstract*—Future low-inertia power systems will introduce challenges to system operators to maintain essential grid services such as fast frequency control (FFC). Hence, there is a need for efficient solutions that can provide the desired FFC capability and arrest high rate-of-change-of-frequency (RoCoF). Recent advancements in information and communication infrastructure within the smart grid concept have created new opportunities to optimally control and utilize the immense potential of thermostatically controlled loads (TCLs), such as refrigerators. However, modeling and controlling different types of TCLs to deliver a precise collective FFC response is challenging. In this regard, this paper develops an adaptive decentralized autonomous fuzzy-temperature-frequency (FTF) control strategy to enable refrigerators to alter their power consumption according to variations in the grid frequency. The ability of the proposed FTF controller to modify the power consumption of a population of refrigerators in accordance with a reference power profile is demonstrated through a set of simulations. The results demonstrate the effectiveness of the proposed controller through a strong improvement in the frequency security parameters, i.e. RoCoF and frequency nadir, and with a negligible impact on the thermodynamic performance of refrigerators.**

***Index Terms*—Ancillary service, fast frequency control, fuzzy-logic control, low-inertia power systems, thermostatic loads**

NOMENCLATURE

Abbreviations

FFC	Fast frequency Control
FLC	Fuzzy Logic Control
FTF	Fuzzy-Temperature-Frequency
GB	Great Britain
HVAC	Heating, Ventilation and Air-Conditioning
PFR	Primary Frequency Response
RoCoF	Rate-of-Change-of-Frequency
TCL	Thermostatically Controlled Load

Symbols

ΔT	Temperature difference [°C]
η	Power energy transmission efficiency
τ	Sampling time [s]
A^{ca-amb}	Area (A) of the thermal contact between cavity and the ambient room [m^2]
A^{ca-ev}	Area (A) of the thermal contact between cavity and the evaporator [m^2]
C	Thermal capacitance [kWh/°C]
$c_v^{ca},\ c_v^{ev}$	Specific heat capacity c_v of cavity and evaporator [$Jkg^{-1}\ °C^{-1}$]
$f^+,\ f^-$	Upper and lower bound of nominal frequency f [Hz]
$m^{ca},\ m^{ev}$	Mass m of cavity and evaporator [kg]
P	Rate of energy transfer to or from thermal mass [kW]
Q	Heat transfer [J]
R	Thermal resistance [°C/kW]
S_F	Final state of switch
S_{H1}, S_{H2}	Switch 1 and 2 for high frequency
S_H	Final output of switch S_{H2} for high frequency
S_{L1}, S_{L2}	Switch 1 and 2 for low frequency
S_L	Final output of switch S_{L2} for low frequency
S_T	Discrete operation state of thermostat switch
T_{amb}	Ambient temperature [°C]
$T_{ca},\ T_{ev}$	Cavity and Evaporator temperature [°C]
T_{db}	Temperature deadband [°C]
$T_{off},\ T_{on}$	Optimally evaluated temperature to turn refrigerator off and on [°C]
T_{set}	Temperature set-point [°C]
U	Heat transfer coefficient [$Wm^{-2}\ °C^{-1}$]
U^{ca-amb}	Heat transfer coefficient between cavity and the ambient room [$Wm^{-2}\ °C^{-1}$]
U^{ca-ev}	Heat transfer coefficient between cavity and the evaporator [$Wm^{-2}\ °C^{-1}$]

This work was supported in part by the Croatian Science Foundation through project Active NeIghborhoods energy Markets pArTicipatION–ANIMATION under Grant IP-2019-04-09164.

Sumit Nema and Vivek Prakash are with the Department of Automation, Banasthali Vidyapith, Tonk, Rajasthan, India (e-mails: sumitnema@live.in; vivekprakashee@gmail.com).

Hrvoje Pandžić is with the University of Zagreb Faculty of Electrical Engineering and Computing, Zagreb, Croatia (e-mail: hrvoje.pandzic@ieee.org).

I. INTRODUCTION

INTEGRATION of inverter-based renewable energy sources into the existing power grids causes a reduction in the overall system inertia, resulting in high-frequency excursions and increased frequency nadir during contingencies. Since FFC provisions [1]–[3] require flexibility and instantaneous switching of the supported devices to arrest frequency nadir, a part of the solution for quick active power delivery are TCLs [4], [5]. TCLs are devices able to automatically adjust their energy consumption based on the grid frequency. A wide range of thermal loads, such as refrigerators or air-conditioning devices, can be used for this cause [6]. Refrigerators use temperature hysteresis controllers, which are resistant to slight temperature changes, enabling them to perform energy arbitrage and provide frequency services [7]. Control algorithms harnessing TCL power for FFC can be categorised as centralised, decentralised and hybrid, each reviewed in the following sections.

A. Centralised Control

Utilizing flexible loads for frequency regulation demonstrates positive outcomes. Study [8] relies on a linear regression model for maximum power characterization. However, its imposed linear relationship between the parameters may overlook complexities and nonlinear behaviour, possibly leading to less accurate outcomes. Furthermore, the centralized control strategy proposed in the paper does not consider dynamic and fluctuating grid conditions, affecting performance and effectiveness. On the other hand, a centralised load following strategy incorporating a population of heterogeneous TCLs can provide aggregate regulation capacities and ramping rates [9]. However, utilization of approximated three-input single-output state-space models and hierarchical centralized control algorithm can compromise system performance, accuracy, and real-time responsiveness in the load following services.

By regulating the internal electrical equipment through a combination of methods, HVAC systems can sustain a consistent reduction in power consumption and generate a steady virtual power output within a specific timeframe [10]. In study [10], a comprehensive centralized-distributed architecture is employed, utilizing chilled water temperature regulation and end air volume regulation techniques to effectively achieve power reduction in HVAC systems. However, it lacks a discussion on potential limitations or drawbacks related to the aggregation and control used to achieve power reduction in HVACs. According to [11], the employing TCLs for PFR can be economically viable. The article's focus on autonomous microgrids limits the generalization of its findings to other energy systems and grid configurations. Paper [12] introduces a framework utilizing refrigerators and distributed energy resources that aims to deliver fast PFR. The framework's emphasis on local objectives is limited by a small-scale experiment with few appliances, requiring further research for scalability and real-world effectiveness.

B. Decentralises Control

Although centralised techniques described above are simple to adopt, they are prone to communication errors [13]. This may cause real-time control systems to become unstable due to a large number of connected heterogeneous devices. To overcome this, the authors in [13] suggest a temperature controller that utilizes refrigerators as flexible loads for reserve provision and demand response, requiring minimal communication infrastructure. An approach with communication delays incorporating model predictive control is discussed in [14], primarily focusing solely on massive inverter air conditioners as flexible regulation resources. In addition, [15], [16] propose approaches that demonstrate accurate modulation of aggregate power consumption and allow for decentralized implementation. In their findings, short-term fluctuations should have less effect on temperature regulation and user comfort, but the works do not delve into potential challenges that may arise when implementing and scaling up. Utilization of domestic refrigerators and industrial bitumen tanks as decentralized frequency-responsive loads in the GB power system is proposed by the authors in [17], [18], where slight discrepancies arose from variations in the initial states of tanks and the randomization of their frequency controllers. A study presented in [19] introduces and analyzes two distinct implementations, namely the frequency linear controller and the preprogrammed controller. It is revealed that the modulation of power consumption of TCLs linearly proportional to the frequency affects the thermodynamic performance and the users' comfort. A decision tree algorithm is developed in [20] that limits the disconnection of loaded feeder due to a maloperation of the under-frequency relays. However, decision trees are prone to overfitting, sensitive to input changes, limited in capturing complex interactions, struggle with continuous variables, and are influenced by data imbalance. Authors in [21] use control of refrigerators without real-time communication and improve frequency stability. In the study presented in [22], a new and reliable stochastic control algorithm is employed to simulate and assess the dynamic behaviour of domestic refrigerators in the context of frequency regulation. Unlike conventional linear and deterministic control algorithms, this stochastic control approach guarantees system stability and addresses the issue of energy payback. The important considerations include activation threshold for stochastic control during frequency drops and addressing concerns about compressor damage by limiting the switching frequency.

C. Hybrid Control

The hybrid and hierarchical control system is identified as a middle ground between the centralised and decentralised approaches. A three-level control architecture is commonly used in the hierarchical control of TCLs [23], [29]. At the highest level, an aggregator first sets the primary reserve requirement to the distribution substations [23]. At the intermediate level, distribution substations dispatch control signals to individual TCLs, after estimating the real-time power availability of TCLs. The final frequency control loop is implemented at the local controller level, enabling TCLs to react to frequency events on their own [23], [30]. However, an aggregator still needs to communicate with individual TCLs, which may be challenging in large systems and could affect the users' comfort. This is incorporated in a two-stage hierarchical TCL scheduling framework in [31] that assumes TCLs can be treated as a virtual battery, potentially overlooking individual TCL behaviours. The focus is on lower-stage TCL scheduling and privacy, lacking coordination discussions across the power system and device levels.

Dynamic demand control can be incorporated into the frequency responsive appliances for the purpose of frequency stability [25]. The need for widespread adoption and coordination among various appliances incorporating dynamic demand control is yet to be addressed. A random switching and cycle recovery method for dynamic TCL control for the PFR and secondary frequency response is proposed in [26], however, the proposed random switching and cycle recovery can lead to inefficient energy usage and higher bills, requiring control strategy optimization. Paper [27] explores the use of real coded genetic algorithms to achieve fast PFR from dynamically controlled space heaters without disrupting their regular operation.

TABLE I
OVERVIEW OF THE EXISTING RESEARCH ON TCLS PROVIDING FFC SERVICES (FR–FREQUENCY RESPONSE; PFR–PRIMARY FREQUENCY RESPONSE; FC–FREQUENCY CONTROL; SFR– SECONDARY FREQUENCY RESPONSE)

Ref. No.	TCL Type	FC Type	Control Strategy	Control Parameters
[4]	Refrigerator	FR	Secondary frequency control via DR	Frequency
[10]	Thermal Load	PFR	Centralized	Power Consumption
[11]	Thermal Load	PFR	Centralized	Frequency
[12]	Refrigerator/Freezer, Electric Heater, Oven	Fast PFR	Centralized Master Controller	Net-Load Management
[15]	Refrigerators	FR	Decentralized Stochastic Control	Power Consumption, Temperature
[16]	Thermal load	PFR	Decentralized, Hardware in the loop	Heat Transfer dynamics, Temperature
[18]	Refrigerators	FR	Decentralized Dynamic Control	Power Consumption
[19]	Refrigerators	PFR	Decentralized, Linear	Power Consumption
[21]	Thermal load	Rapid	Linear, Pre-Set Shape Controller	Frequency
[22]	Refrigerators	PFR	Decentralized Stochastic Control	Temperature probability
[23]	Air conditioners, Electric water heaters	PFR	Three Level Hierarchical Control	Available Power, frequency
[24]	Thermal load	FR	Deterministic	Frequency
[25]	Refrigerators	FC	Dynamic Demand Control	Temperature
[26]	HVAC, Electric water heaters	PFR, SFR	Dynamic Demand Control	Demand Profile, Load Rebound
[27]	Space Heaters	Fast PFR	Dynamic Control, Lead-lag Controller	Indoor Temperature, Grid Frequency
[28]	Refrigerators, Air conditioners, Heat Pump	PFR	Direct Load Control	Temperature

Nevertheless, genetic algorithms have complexity, parameter sensitivity, and may converge prematurely.

Challenges of a real-time energy balance of a population of refrigerators using stochastic Markov chain models and Kalman filtering for both state and joint parameter/state estimation are discussed in [25], [32], [33]. Similarly, a transition modelling technique is used to characterise the dynamic behaviour of aggregated TCLs [24]. Implementing real-time monitoring and control of appliances requires advanced sensors, communication infrastructure, regulatory adjustments, and changes in business models. Reference [28] estimates the technical resource potential of TCLs for short-duration balancing services. However, the dynamics and adaptability of individual refrigerators for frequency control without undermining their operational regimes must be fulfilled. Therefore, the European Network of Transmission System Operators for Electricity (ENTSO-E) framed a guideline for thermal loads to participate in grid frequency support [34].

Table I summarizes the reported literature on TCLs for different devices, parameters, control strategies, and control parameters. Based on the literature review on various TCL control strategies for grid frequency control, the following research gaps are identified: (i) abrupt on-off switching control may disturb the system performance, (ii) the threshold control strategy tends to synchronize cooling cycles of the participating appliances, (iii) complexity and the computational burden for deploying reserves should be minimized, (iv) aggregation evolution and methodologies should be implementable to the standard and large power system, (v) the random switching and cycle recovery must be accompanied as per regulatory framework and without undermining users' comfort, (vi) control schemes should be scalable, adaptable and generalized to all TCLs to meet proper performance indices.

To address the aforementioned requirements, an adaptive and intelligent control strategy with decentralised control may be used. An intelligent control strategy can be adopted using FLC, incorporating human expert knowledge into the design of nonlinear controllers [35]. By utilizing the FLC principles, which the traditional control theory is unable to address, qualitative and heuristic factors can be applied for control purposes in a systematic manner [36]. FLC can handle nonlinearity, deal with erroneous inputs, and offer higher-than-average disturbance insensitivity without the need for a precise mathematical model. In complicated, nonlinear, or undefinable systems, the FLC typically outperforms other controllers when good empirical knowledge is available. If such properties are intended, fuzzy control theory can be rigorous and fuzzy controllers can have exact and analytical structures with guaranteed closed-loop system stability in compliance to performance standards e.g. time, error, stability, tolerance. While previous works e.g. [37]–[39] have explored an adaptive FLC for frequency regulation in contexts of secondary controller design in LFC, droop control incorporating renewable energy, control of battery energy storage system for LFC, etc., the adaptation of the proposed control strategy to refrigerator systems represents a significant contribution. To optimize frequency control via refrigerators, a sequential approach is adopted based on system frequency and cavity temperature characteristics. Switching off and on of the refrigerator is determined by the cavity temperature values and by frequency deviations. A precise and accurate adaptive fuzzy mechanism is designed for both frequency and temperature to simultaneously comply with the provision standards and regulations, without undermining the performance of the devices.

To address the outlined research challenges the main contribution of this paper is twofold:

1) Development of a rigorous and precise frequency responsive switching control strategy structured with performance specifications to provide accurate and reliable FFC reserves using refrigerators.
2) To assess feasibility of the developed refrigerator controller to handle the post-fault frequency dynamics, *i.e.* RoCoF and frequency deviation.

The rest of the paper is organized as follows. Section II discusses the generalized model of TCLs, conventional control methods, and the mandatory provision for TCLs. In addition, the integrated control of a refrigerator is explained, focusing on the Fuzzy-Temperature-Frequency (FTF) control strategy.

Section III describes the case study, including the refrigerator model and the GB system for performance evaluation. Section IV includes simulation results and analysis. Finally, relevant conclusions are drawn and discussed in Section V.

II. Control Framework

A. Generalized model of TCLs

An aggregation of TCLs is comprised of multiple units with aggregated power. The system thermodynamics is modeled by two state variables, the discrete operation state S_T and the cavity temperature of the conditioned mass T_{ca}. A first-order ordinary differential equation described by Eq. (1) is modeled for the aggregation of N TCLs [9].

$$\frac{\mathrm{d}T_{ca,j}(t)}{\mathrm{d}t} = \frac{1}{C_j R_j}\left(T_{amb,j}(t) - T_{ca,j}(t) - S_{T,j}(t) R_j P_j\right), \quad (1)$$

where $j = 1, 2 \ldots, N$; $C_j = (c_{v,j} \times m_j)$; $R_j = (\frac{1}{U_j \times A_j})$, and $S_{T,j}$ is the operation state governed by a thermostatic switching logic constraint by a predetermined temperature deadband given as:

$$S_{T,j} = \begin{cases} 0 & T_{ca,j}(t) < T^{\min}_{ca,j}, \\ 1 & T_{ca,j}(t) > T^{\max}_{ca,j}, \end{cases} \quad (2)$$

where $T^{\max}_{ca,j}$ and $T^{\min}_{ca,j}$ are the upper and lower bounds of the temperature and evaluated as follow:

$$T^{\min}_{ca,j} = T_{set,j} - \frac{T_{db,j}}{2}, \quad T^{\max}_{ca,j} = T_{set,j} + \frac{T_{db,j}}{2}. \quad (3)$$

The steady-state cooling time $T_{c,j}$ and the heating time $T_{h,j}$ for the j^{th} TCL are determined as follows:

$$T_{c,j} = C_j R_j \ln\left(\frac{P_j R_j + T^{\max}_{ca,j} - T_{amb,j}}{P_j R_j + T^{\min}_{ca,j} - T_{amb,j}}\right), \quad (4)$$

$$T_{h,j} = C_j R_j \ln\left(\frac{T_{amb,j} - T^{\min}_{ca,j}}{T_{amb,j} - T^{\max}_{ca,j}}\right). \quad (5)$$

Output power of an aggregation of all TCLs $P_T(t)$ is obtained as:

$$P_T(t) = \sum_{j=1}^{N} \frac{1}{\eta_j} S_{T,j}(t) P_j. \quad (6)$$

Since the control input for each TCL is its setpoint temperature $T_{set,j}$, which might have different operating and acceptable limits as per consumer's comfort and application, it also satisfies the constraint:

$$T^{-}_{set,j} \leq T_{set,j} \leq T^{+}_{set,j}. \quad (7)$$

Here, $T^{-}_{set,j}$ and $T^{+}_{set,j}$ are the lower and upper bounds of the acceptable thresholds for the TCL.

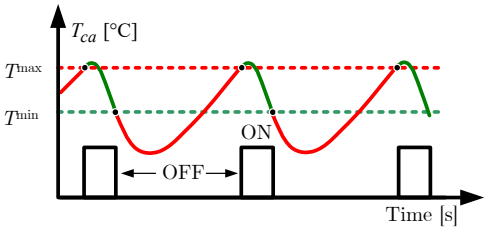

Fig. 1. Generalized cavity temperature T_{ca} [°C] of a refrigerator followed by a compressor on/off status.

B. Essential requirements

1) Conventional Control: The manufacturer or the owner has to specify set points for the temperature in the food storage compartment. Fig. 1 shows the switching operation of a compressor along with the cavity temperature T_{ca}. The thermostatic controller continuously measures T_{ca} and compares it with the thresholds $T^{\min}$ and $T^{\max}$ to generate S_T as per Eq. (2). Since heat transfer through the thermal contact between the evaporator and the cavity takes some time, there is a delay in the temperature decrease. The compressor switches off once T_{ca} reaches the threshold $T^{\min}$. However, there is a further drop in T_{ca} before it starts to increase due to the heat transfer process. The compressor remains off until T_{ca} reaches $T^{\max}$ again.

2) Mandatory provision for TCLs: The essential frequency response service for TCLs prescribes a provision of the T_{set} adjustment based on the system frequency [34] considering a deadband around $f = 50$ Hz that keeps the temperature unaffected. If the grid frequency violates the prescribed deadband, the TCLs must adjust their set-points proportionate to the grid frequency variation. The interval for frequency deadband is $[f^-, f^+]$, where $f^- \leq f \leq f^+$. TCLs must adjust their T_{set} points in proportion to the frequency deviations. At the statutory limits of the system frequency range $\left[f^{\min}, f^{\max}\right]$, the limits of the controllable setpoint range $\left[T^{\min}_{set}, T^{\max}_{set}\right]$ should be reached and should cover at least half of the hysteresis interval $\left[T^{\min}, T^{\max}\right]$. For cooling appliances, this results in a functional requirement visually depicted in Fig. 2. A converse approach should be adopted for heating systems. The code also mandates that the frequency is sampled at least once every 0.2 seconds, accurately to 0.05 Hz in the steady state, and with a sensitivity to fluctuations of 0.01 Hz.

$$T_{set}(f) = \begin{cases} T^{\max}_{set}, & f \leq f^{\min}, \\ \bar{T}_0 + \frac{(T^{\max}_{set} - \bar{T}_0)(f^- - f)}{f^- - f^{\min}}, & f^{\min} < f < f^-, \\ \bar{T}_0, & f^- \leq f \leq f^+, \\ \bar{T}_0 + \frac{(T^{\min}_{set} - \bar{T}_0)(f - f^+)}{f^{\max} - f^+}, & f^+ < f < f^{\max}, \\ T^{\min}_{set}, & f \geq f^{\max}. \end{cases} \quad (8)$$

C. Integrated control of a refrigerator

The developed FTF refrigerator control scheme is provided in Fig. 3. The temperature controller measures the cavity temperature T_{ca} and generates thermostat switch status S_T as per Eq. (2). Grid frequency f is measured and examined whether

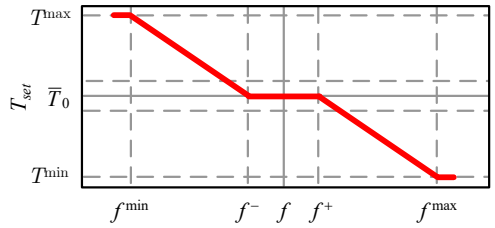

Fig. 2. Relationship between T_{set} and f for cooling TCLs

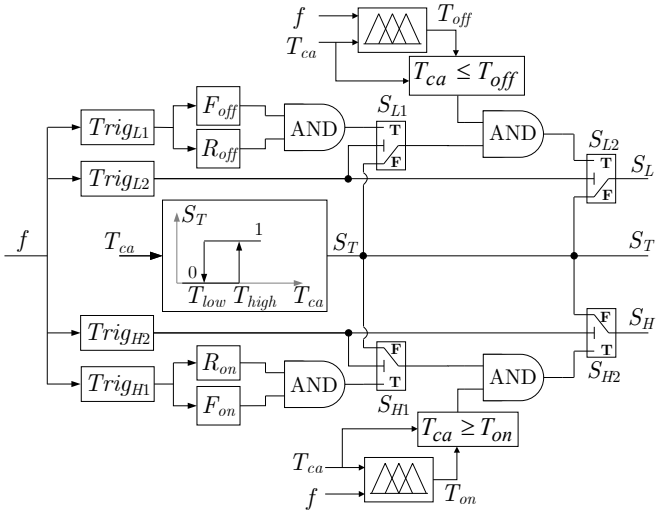

Fig. 3. The proposed adaptive FTF controller depicting the proposed triggering, local hysteresis controller and FLC scheme.

it is within the threshold interval $[f^- : 49.98,\ f^+ : 50.02]$. For a frequency drop below lower frequency threshold f^-, trigger $Trig_{L1}$ (triggering 1 for a low-frequency event) generates output as per Eq. (9). When $Trig_{L1}$ is 1, frequency off signal $F_{off} : [0, 1]$, is generated as per Eq. (13), which confirms a continuous drop in frequency. Simultaneously, the cavity temperature of the refrigerator is confirmed using Eq. (15). The output of the refrigerator off signal, $R_{off} : [0, 1]$ indicates that the refrigerator is on and cooling. The output of F_{off} and R_{off} is passed on to the AND logic, which validates that for a drop in both f and T_{ca}, the refrigerator is ready to turn off. $Trig_{L2}$ (triggering 2 for a low-frequency event) is defined in Eq. (11). It enables the operation of switch S_{L1} and connects to position **T** (true), which is normally connected to position **F** (false). Output signal $S_{L1} = 1$ from position **T** is taken at $Trig_{L2}$. A similar but converse approach is applied to turn on the refrigerator in case of an increase in frequency, which generates $S_{H1} = 1$, indicating the refrigerator is ready to switch on.

$$Trig_{L1} = \begin{cases} 1, & f < f^-, \\ 0, & \text{otherwise}, \end{cases} \tag{9}$$

$$Trig_{H1} = \begin{cases} 1, & f > f^+, \\ 0, & \text{otherwise}, \end{cases} \tag{10}$$

$$Trig_{L2} = \begin{cases} 1, & f <= f^-, \\ 0, & \text{otherwise}, \end{cases} \tag{11}$$

$$Trig_{H2} = \begin{cases} 1, & f >= f^+, \\ 0, & \text{otherwise}, \end{cases} \tag{12}$$

$$F_{off} = \begin{cases} 1, & \text{if } f(t) - f(t-\tau) < 0 \text{ for } Trig_{L1} = 1, \\ 0, & \text{otherwise}, \end{cases} \tag{13}$$

$$F_{on} = \begin{cases} 1, & \text{if } f(t) - f(t-\tau) > 0 \text{ for } Trig_{H1} = 1, \\ 0, & \text{otherwise}, \end{cases} \tag{14}$$

$$R_{off} = \begin{cases} 1, & \text{if } T_{ca}(t) - T_{ca}(t-\tau) < 0 \text{ for } Trig_{L1} = 1, \\ 0, & \text{otherwise}, \end{cases} \tag{15}$$

$$R_{on} = \begin{cases} 1, & \text{if } T_{ca}(t) - T_{ca}(t-\tau) > 0 \text{ for } Trig_{H1} = 1, \\ 0, & \text{otherwise}. \end{cases} \tag{16}$$

Since T_{ca} varies based on the refrigerator type, size, and efficiency, turning refrigerators off and on for frequency control should be sequential instead of switching them off/on simultaneously. The number of refrigerators participating in frequency control is directly proportional to the frequency deviation. Following a drop in frequency, the refrigerators are switched off starting from the one with the lowest T_{ca}. On the other hand, in case of a frequency rise, the refrigerators are switched on starting from the one with the highest T_{ca}. Howbeit, for a severe under-frequency deviation, multiple refrigerators might be switched off simultaneously. Further, it is required to minimize the number of refrigerators that might switch on at the same time after being switched off following a frequency drop. For this purpose, an adaptive and autonomous fuzzy mechanism is adopted which decides the specific cavity temperature T_{off} for a frequency drop for an individual refrigerator after a mandatory service provision, as discussed in Section II-B2.

D. Fuzzy-Temperature-Frequency (FTF) control strategy

An adaptive FLC is an efficient approach to control nonlinear uncertain systems [35], [36]. Fig. 4 shows a general structure of an FLC system that contains four processing units: a fuzzifier (to obtain a fuzzy input value from a crisp input), a fuzzy rule base, a rule-based system, *i.e.* an inference mechanism (to obtain fuzzy output), and a defuzzifier (to obtain a crisp output from a fuzzy output) [40].

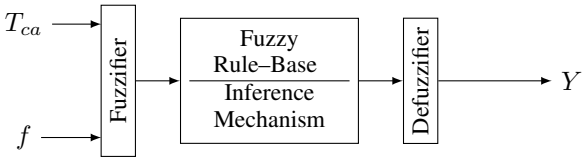

Fig. 4. Dynamic structure of a FLC depicting both inputs, the processing units and the corresponding output.

Both the linguistic values (defined by the fuzzy sets) and the crisp (numerical) data can be used as inputs for a fuzzy system.

Linguistic variables in fuzzy logic are labels representing imprecise concepts, allowing for intuitive reasoning by assigning linguistic terms to degrees of membership within fuzzy sets, bridging human perception and computational reasoning. The Mamdani reasoning [41] is implemented for the inference mechanism. Input signals T_{ca} and f are merged and fuzzy rules are implemented to determine optimal T_{off} and T_{on} values. Database (which includes a summary of the inputs and the output to make a fuzzy set) and rules form an interference connection. The rule base is the control approach of the system. Two trapezoidal and three triangular membership functions for the inputs and the output of the FTF strategy are proposed in Fig. 5.

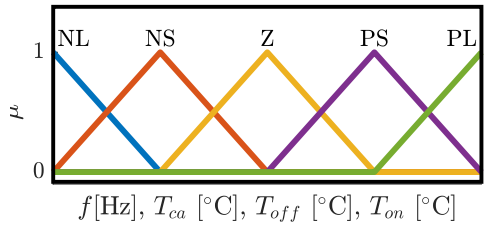

Fig. 5. Designed membership function for inputs and outputs followed by linguistic variables.

The operating range of the fuzzy input variables is $f : [50, 50.8]$ for the frequency rise, $f : [49.2, 50]$ for the frequency drop, while the cavity temperature range is $T_{ca} : [7.5, 8.5]$. Linguistic variables, as described in [42], for the input and output fuzzy subsets are as follows: PL is positive large, PS is positive small, Z is zero, NS is negative small, NL is negative large. The applied rule can be read as 'if T_{ca} is NL and f is NL, THEN Y is PL'.

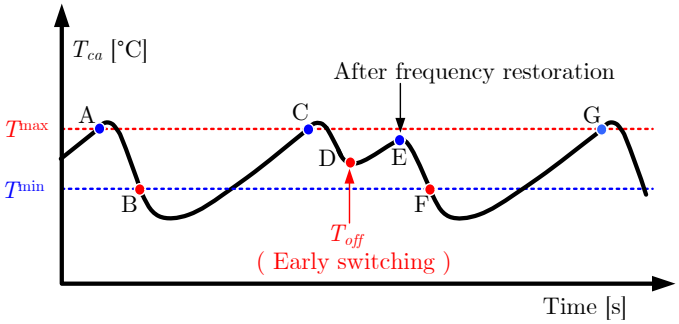

Fig. 6. Early switching strategy to determine optimal temperature T_{off} to turn a refrigerator off for a drop in system frequency.

To minimize the abrupt switching of refrigerators during/pre/post fault events including the door opening effects, it is desired to set specific T_{off} and T_{on} for each refrigerator. To overcome this, rules for the FTF control are created depending on the variation of T_{ca}, as shown in Fig. 6–7 for early switching the refrigerator off and on. Following a drop in frequency, refrigerators need to be switched off starting from the one with the lowest T_{ca}. In Fig. 6, A, C, and G are the points where a refrigerator switches on, while B and F are the switching-off points. For a drop in the system frequency, a refrigerator needs to be switched off before the minimum temperature threshold. Point D is the T_{off} that will be decided by the FTF controller following the mandatory provision. From D to E, T_{ca} will start rising and, after the frequency restoration at point E, the conventional operation will continue.

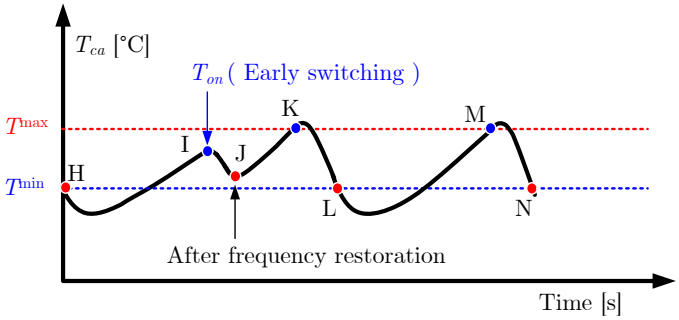

Fig. 7. Early switching strategy to determine optimal temperature T_{on} to turn a refrigerator on for a rise in system frequency.

Similarly, following a rise in frequency, refrigerators need to be switched on starting from the one with the highest T_{ca}. For a rise in the system frequency, the refrigerator will be switched on before the maximum threshold. In Fig. 7, H, L, and N are the points where the refrigerator switches off, while K and M are the switching-on points. The point I corresponds to T_{on}. From I to J, T_{ca} will start decreasing and, after the frequency restoration at point J occurs, the conventional operation will continue. The fuzzy linguistic output is obtained by the fuzzy inference mechanism using the rules listed in Table II.

TABLE II
RULE-BASE FOR THE FTF OUTPUT

Y		f [Hz]				
		NL	NS	Z	PS	PL
T_{ca} [°C]	NL	PL	PL	PS	PS	Z
	NS	PL	PS	PS	Z	NS
	Z	PS	PS	Z	NS	NS
	PS	PS	Z	NS	NS	NL
	PL	Z	NS	NS	NL	NL

The results obtained from the rules are forwarded for defuzzification. The modified crisp value is obtained as:

$$Y = \frac{\sum_{i=1}^{n} c_i \cdot \mu(c_i)}{\sum_{i=1}^{n} \mu(c_i)}, \tag{17}$$

where n is the number of the fuzzy set for the discrete function, and $\mu(c_i)$ is the membership value for point c, which is a crisp value of membership function. T_{off} and T_{on} can be obtained using Eq. (17). Hence, the proposed FTF strategy determines the optimal T_{off} and T_{on} with the self-adaptive capability, following the prescribed and mandatory thresholds of T_{ca} and f. The FTF controller output is further compared with the cavity temperature. $T_{ca} \leq T_{off}$ implies the refrigerator could be turned off. Its output [0,1] is passed on to another AND logic and switch status S_L is generated through the switch S_{L2}, which enables at $Trig_{L2}$, as per Eq. (11). $S_L = 1$ implies that the refrigerator is ready to switch off. A similar method is adopted for a frequency increase to

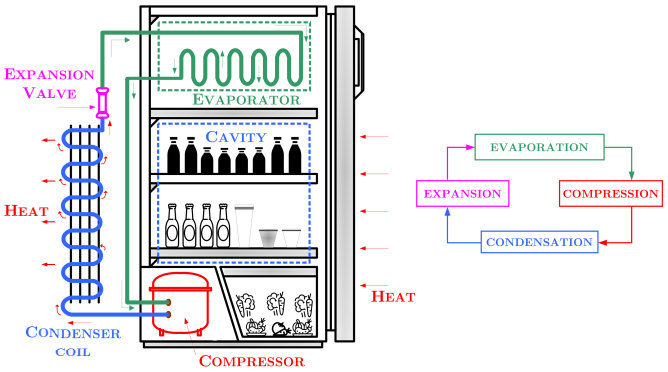

Fig. 8. A typical domestic refrigerator depicting general assembly and the processing cycle: evaporation, compression, condensation and expansion.

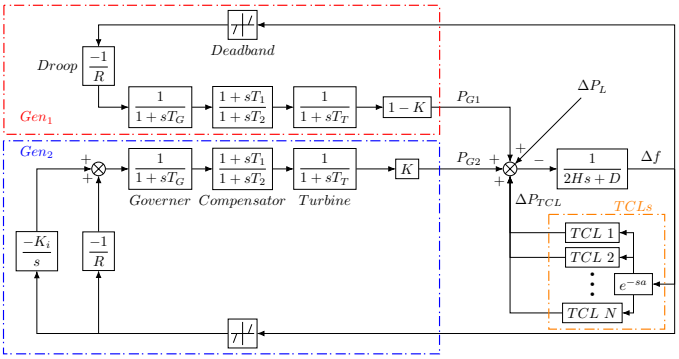

Fig. 9. Generalized model of the GB system with integrated refrigerators and communication delays.

generate S_H. Operation of the coordinated TCLs is managed by the final status of switch S_F determined by Eq. (24).The refrigerator's control strategy takes into account user comfort and the thermodynamic properties, resulting in the complete absence of rebound effect.

III. Case Study Description

A. Thermodynamic model of refrigerators

Residential refrigerators generally incorporate two thermal compartments, the cavity, and the evaporator. A compressor mounted to the evaporator dissipates heat to the environment. The thermal contact between the cavity and the evaporator, as well as between the cavity and the environment, enables heat transfer as depicted in Fig. 8. To model the thermodynamic performance of refrigerators, first-order differential equations are used:

$$\frac{\mathrm{d}Q}{\mathrm{d}t} = -U \times A \times \Delta T, \tag{18}$$

$$\frac{\mathrm{d}T_{mass}}{\mathrm{d}t} = \left(\frac{\mathrm{d}Q}{\mathrm{d}t}\right) \div (c_v \times m)\,. \tag{19}$$

The evaporator and cavity are modeled separately based on Eqs. (20) and (21). T_{amb} is set to 22°C, while temperature interval $\left[T^{\min}, T^{\max}\right]$ is set to [7.5, 8.5]. A similar model is used for the freezer compartment of the refrigerator, which is also modeled having temperature interval [-15, -16]. Parameters of Eqs. (20)–(21) are taken from [43]. Power consumption of one refrigerator is 0.1 kW.

B. Power system description

The steady-state GB system includes a total of 29 nodes (bus bars), 24 synchronous generators and 22 wind farms with total generation of 60.29 GW and 63 constant impedance loads of 59.84 GW [44]. Single-line diagram is depicted in Fig. 10.

A simplified GB power system dynamic model is mainly used to demonstrate the impact of a declining system inertia on primary frequency control, as in e.g. [45], and also to assess feasibility of the proposed control strategy for a large system. In the case study, we use a single-area GB power system model shown in Fig. 9. The base demand is 20 GW. An inertia constant of 6.5 s was estimated due to an inter-connector failure that occurred on September 28, 2012. The observed total in-feed loss was 1000 MW, while the maximum and minimum RoCoF over 500 ms were 0.168 Hz/s and 0.116 Hz/s [46]. Inertia constant H is set to 6.5 s, however, this value will decrease in the future grids due to an increasing penetration of renewable energy sources [47]. The influence of frequency-dependent load is modeled by a damping constant $D = 1$ [p.u.]. Two aggregated generators are modeled, Gen_1 capable of providing PFR only, while Gen_2 is used for both the primary and the secondary frequency responses. $K = 80\%$ is used to segregate Gen_1 and Gen_2. A governor droop characteristic of 3-5% for the provision of the primary frequency control is essential for large generators [48]. Governor droop characteristic is modeled with gain $1/R$ for $R = 0.05$. $T_G = 0.2$ s represents the governor's time constant. To ensure stable performance of the frequency control, a transient droop compensator is incorporated with time constants $T_1 = 2$ s and $T_2 = 20$ s. Mechanical power generated from the turbine has a time constant $T_T = 0.3$ s. Supplementary control coefficient K_i is set to 0.05 [47]. e^{-sa} is the communication delay for the TCLs where a is the step size. Based on Fig. 9, the system frequency dynamics can be expressed as:

$$\Delta f(s) = \frac{P_{G1}(s) + P_{G2}(s) + \Delta P_{TCL}(s) - \Delta P_L(s)}{2Hs + D}. \tag{22}$$

where P_{G1} and P_{G2} are the outputs of aggregated generators Gen_1 and Gen_2. ΔP_{TCL} is the total available power involving frequency control for a loss of a generation of ΔP_L. The total power consumption of the refrigerator is expressed as:

$$P_{TCL} = \sum_{j=1}^{N} P_j S_{F,j}. \tag{23}$$

Operation of the coordinated refrigerators is managed by the final status of switch S_F corresponding to:

$$S_{F,j} = \begin{cases} 0, & \forall\ S_{L,j} = 1, \\ 1, & \forall\ S_{H,j} = 1, \\ S_{T,j}, & T^{\min}_{ca,j} \le T_{ca,j} \le T^{\max}_{ca,j}. \end{cases} \tag{24}$$

IV. Simulation Results and Analysis

The simulation results are presented under two subsections which first assess the proposed FTF controller and then

$$\frac{\mathrm{d}T_{ev}(t)}{\mathrm{d}t} = \frac{U^{ca-ev} \times A^{ca-ev}}{c_v^{cv} \times m^{ev}} \left(T_{ca}(t) - T_{ev}(t)\right) - \frac{P \times S_F}{c_v^{ev} \times m^{ev}}, \tag{20}$$

$$\frac{\mathrm{d}T_{ca}(t)}{\mathrm{d}t} = \frac{U^{ca-amb} \times A^{ca-amb}}{c_v^{ca} \times m^{ca}} \left(T_{amb}(t) - T_{ca}(t)\right) - \frac{U^{ca-ev} \times A^{ca-ev}}{c_v^{ca} \times m^{ca}} \left(T_{ca}(t) - T_{ev}(t)\right). \tag{21}$$

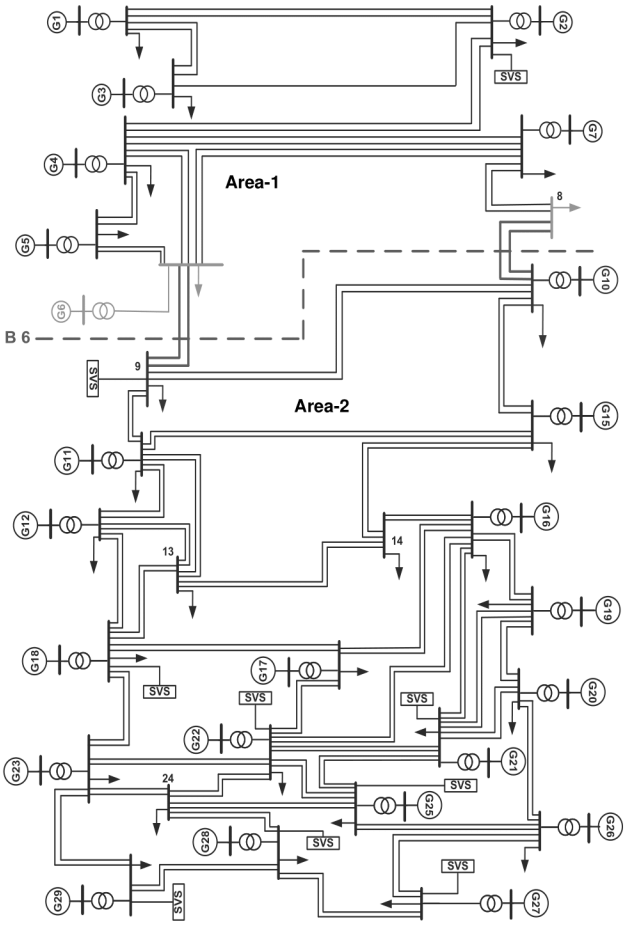

Fig. 10. Single-line diagram of GB power system [44]

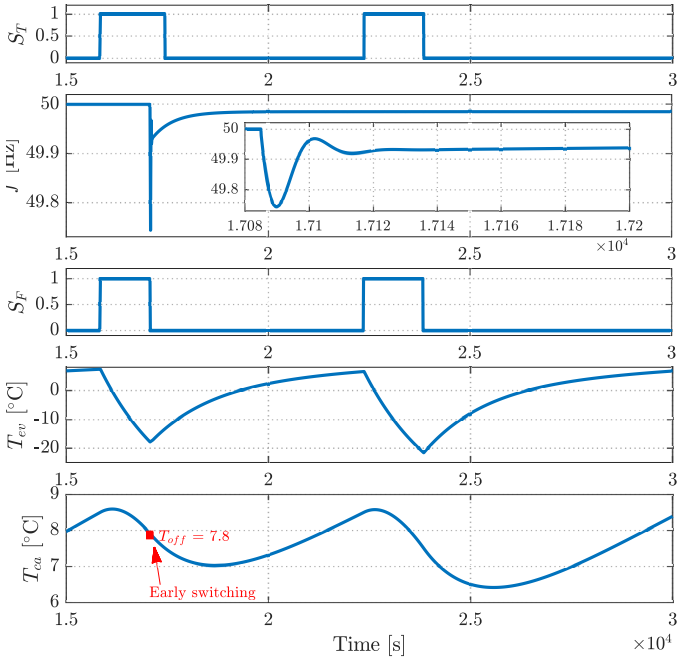

Fig. 11. Activation and performance of the FTF controller depicting operation of S_T, activation of FTF via S_F for early switching, and respective changes in T_{ev} [°C], and T_{ca} [°C].

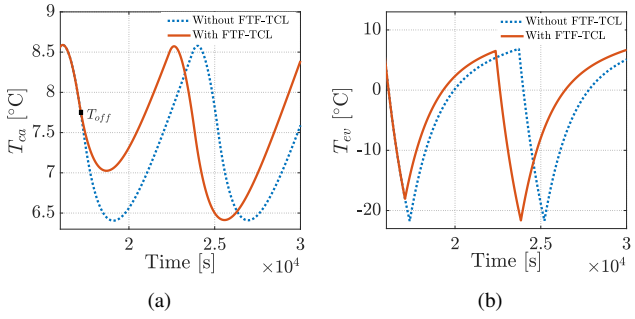

Fig. 12. Comparative analysis of the same refrigerator for (a) T_{ca} [°C], and (b) T_{ev} [°C].

demonstrate the effectiveness of the deployment of refrigerators to provide FFC. Multiple aggregations of refrigerators are considered for simulation. All refrigerators within an aggregation are considered to be homogeneous while the aggregations differ by cavity temperature. To represent the population of refrigerators, parameters of Eqn. (20)–(21) are scaled accordingly. A similar approach for the aggregations of refrigerators has already been considered in [13], [21], [25]. Our work aggregates homogeneous refrigerators with varying T_{ca}. The MATLAB/Simulink platform is used for all simulations.

A. Assessment of the FTF controller

In this case, a loss of 1320 MW of generation is triggered causing a drop in the system frequency to 49.6 Hz. An aggregation of 6.4 million refrigerators operating at the same cavity temperature participate in the FFC to minimize frequency perturbations. Refrigerators can quickly respond to grid power requests, ensuring 50% fulfillment within 15 seconds and sustained power deviation for up to 1 hour [13], therefore a total of $\Delta P_{TCL} = 640$ MW of power is deployed to the system resulting in an improvement in the frequency nadir and RoCoF. Early switching to turn the refrigerators off was found to be $T_{off} = 7.8$ °C.

Switching statuses of S_T and S_F in Fig. 11 clearly exhibit the switching off of refrigerators after a drop in frequency. Consequently, T_{ev} starts increasing instantly, while a rise in T_{ca} is delayed due to the heat transfer process. Hence,

TABLE III
FTF OUTPUT TO FREQUENCY EVENTS

$f = 49.62$[Hz]		$f = 50.47$[Hz]		$T_{ca} = 7.80$[°C]		$T_{ca} = 8.20$[°C]	
T_{ca}[°C]	T_{off}[°C]	T_{ca}[°C]	T_{on}[°C]	f[Hz]	T_{off}[°C]	f[Hz]	T_{on}[°C]
7.59	7.86	7.59	8.33	49.95	7.66	50.05	8.34
7.67	7.86	7.67	8.33	49.90	7.69	50.10	8.31
7.79	7.83	7.79	8.30	49.85	7.71	50.15	8.28
7.86	7.80	7.86	8.27	49.80	7.72	50.20	8.27
7.94	7.77	7.94	8.24	49.75	7.75	50.25	8.24
8.13	7.69	8.13	8.19	49.65	7.80	50.35	8.20
8.21	7.65	8.21	8.15	49.55	7.85	50.45	8.16
8.29	7.62	8.29	8.12	49.45	7.84	50.55	8.16
8.37	7.62	8.37	8.12	49.35	7.88	50.65	8.12

the status of S_T remains 1 until the lower threshold of T_{ca} is reached. After the frequency is restored within the deadband, the operation of S_F is switched back to S_T, which does not undermine the thermodynamic cavity and evaporator performance (Fig. 12(a)–12(b)). A large variation in T_{ev} is due to the constant ambient temperature throughout the simulation [43], [49].

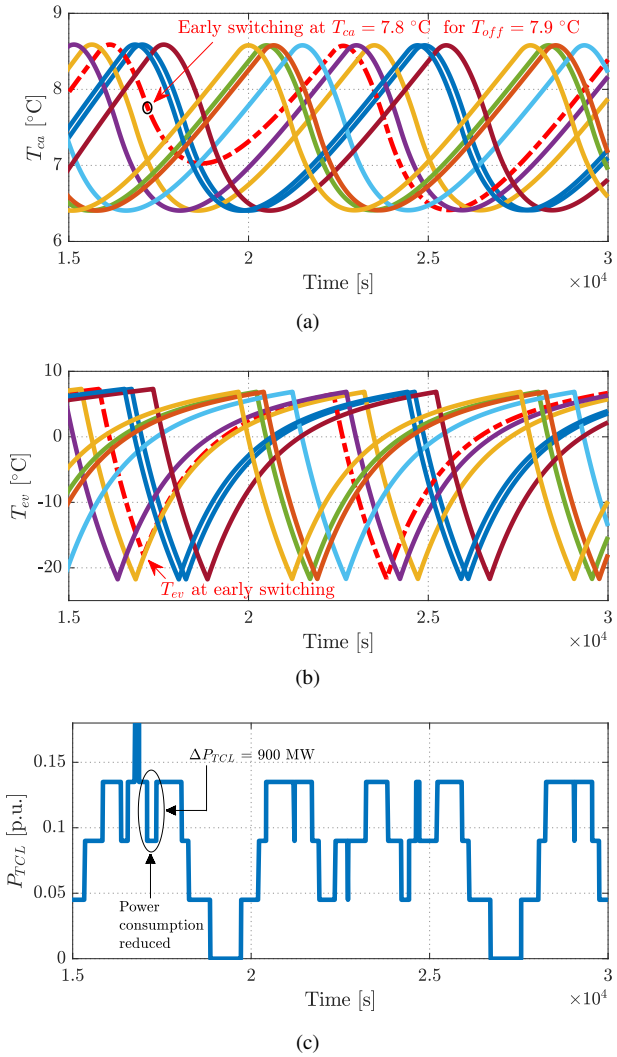

Fig. 13. (a) T_{ca} [°C], (b) T_{ev} [°C] and (c) P_{TCL} [p.u.] of the aggregated refrigerators.

The next analysis considers 10 aggregated homogeneous refrigerators operating at different cavity temperatures. For a loss of generation that causes a frequency drop, different T_{off} are obtained and presented in Table III. Similarly, for a rise in the system frequency, different T_{on} are obtained. In the second half of Table III, T_{off} and T_{on} are obtained for an aggregation of refrigerators for the different system frequency drop and rise magnitudes. Analysis of the temperatures in Table III demonstrates the sequential early switching of refrigerators rather than simultaneous switching as each aggregation has different T_{off} and T_{on} (because of the difference in the cavity temperature). For a drop in frequency, all the refrigerators having $T_{ca} \leq T_{off}$ participate in the frequency restoration. Furthermore, a refrigerator can act quickly to provide FFC service, if the magnitude of frequency deviation is large. The proposed strategy avoids flapping between refrigerator operation modes during a frequency event. The output of the FTF controller for T_{off} and T_{on} is disabled once the refrigerator participates in frequency control up to the frequency restoration or temperature thresholds.

B. FFC from refrigerators

Simulations are carried out to assess the designed controller in case of a 1800 MW loss of generation, expected in the GB system [46]. The frequency nadir should be within 49.2 Hz and the RoCoF should not be greater than the permissible limit of 1 Hz/s using a 500 ms measuring window anywhere in the system [21], [50]. Each of the 10 considered aggregations is composed of 9 million refrigerators.

First, we present the frequency response for all generators committed to the PFR only (without secondary control). Fig. 13(a)–13(b) show the operating profile of 10 refrigerator aggregations after the 1.8 GW generation loss at time $t = 1.7085 \times 10^4$ s. The aggregation of refrigerators participating in frequency control is shown by the red dash-dot trace. T_{ca} [°C] of this aggregation was below $T_{off} = 7.9$ °C (generated by the FTF controller) and is thus turned off before reaching its $T^{\min}$, contributing with $\Delta P_{TCL} = 900$ MW to the grid immediately. Another aggregation (shown by the yellow trace) seems to have a similar T_{ca} profile but it was already turned off as it reached it $T^{\min}$ before the loss of generation. All other aggregations did not follow the criteria of Eqn. (13)–(16), and therefore did not take part in frequency control. However, if the frequency imbalance is more severe, an additional set of aggregations will participate in the FFC if the controller criteria are fulfilled. For the system without the integrated refrigerators, a sudden loss of generation causes the frequency drop to $f_{nadir} = 49.37$ Hz, while the deployment of 900 MW power from the refrigerator aggregation limits the drop to $f_{nadir} = 49.79$ Hz, which is a significant improvement. Also, the RoCoF is improved from 0.164 Hz/s to 0.053 Hz/s.

In our next analysis, the performance of the refrigerator aggregation response is evaluated for the system with segregation of Gen_1 and Gen_2, which includes the mandatory provision of primary and secondary control. A loss of 1.8 GW of generation leads to a drop in the frequency to 49.14 Hz, implying the system operator has to curtail a part of the load with immediate effect. However, refrigerators significantly contribute in this case, resulting in an improvement of 0.42

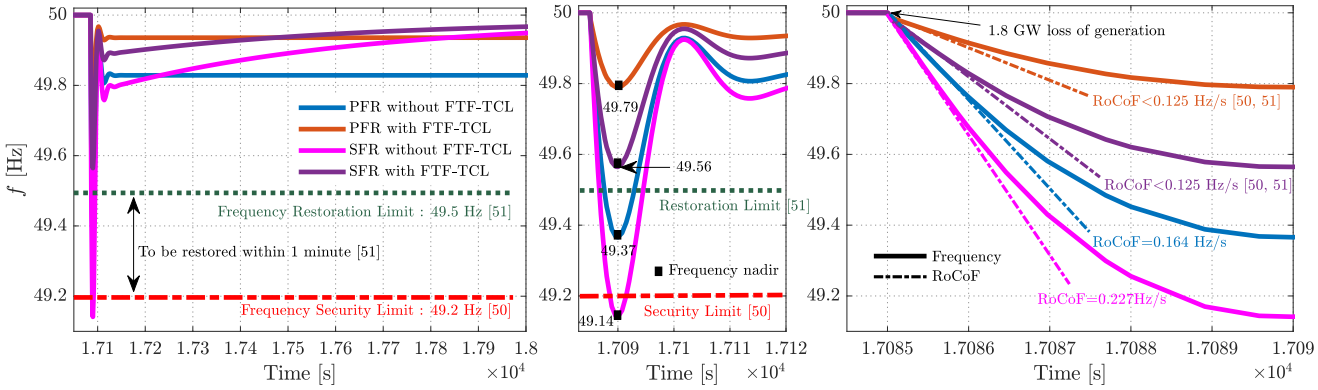

Fig. 14. Frequency response with standards [50], [51], nadir and RoCoF analysis in compliance to the GB system.

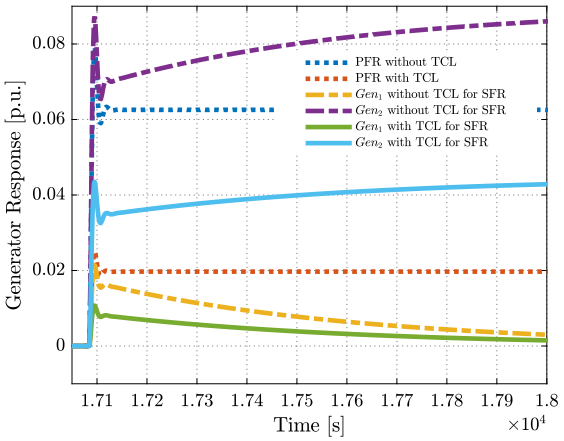

Fig. 15. Generators' response to different operating conditions.

TABLE IV
FREQUENCY ASSESSMENT (PFR–PRIMARY FREQUENCY RESPONSE; SFR– SECONDARY FREQUENCY RESPONSE)

Frequency Response	RoCoF [Hz/s]	f_{nadir} [Hz]	$f^{steady-state}$ [Hz]
PFR (Without FTF-TCL)	0.164	49.37	49.82
PFR (With FTF-TCL)	0.0537	49.79	49.93
SFR (Without FTF- TCL)	0.227	49.14	49.98
SFR (With FTF-TCL)	0.113	49.56	49.98

Hz bringing f_{nadir} to 49.56 Hz. The frequency response in compliance to provisions [50], [51] is depicted in Fig. 14, while the obtained performance parameters are listed in Table IV. The analysis of the performance of the aggregated generators presented in Fig. 15 indicates that the participation of refrigerators reduces the required response of the generators, which reduces the requirement of costly spinning reserves.

To verify and better position the obtained results, the proposed FTF-control strategy is compared with the control strategy adopted in [17], [43]. Switching status of S_F and S_T with temperature T_{ca} and T_{ev} are obtained as depicted in Fig. 16–17. The zoomed plot of the depicted results exhibits the difference and superiority of the proposed FTF-control, which possesses accurate on-off switching while deploying reserve to the grid once activated. Refrigerator aggregation remains off up to the frequency restoration for the FTF-control, as compared to the existing strategy and strictly following Eq. (24). For the existing control of [17], [43], an abrupt switching on of the refrigerator aggregation incident for a short duration appeared and again gets switched off (refer S_F status and T_{ev} variation). This deviation resulted in a delay in the next switching cycles of the refrigerators for normal conditions. Since the refrigerators instantaneously switched on back, the deployed reserve was reduced hence causing higher f_{nadir} and longer settling time as compared to the proposed FTF-control. Frequency dynamics are also obtained for refrigerators having communication delay, as shown in Fig. 17. The proposed control exhibits promising outcomes in this case as well.

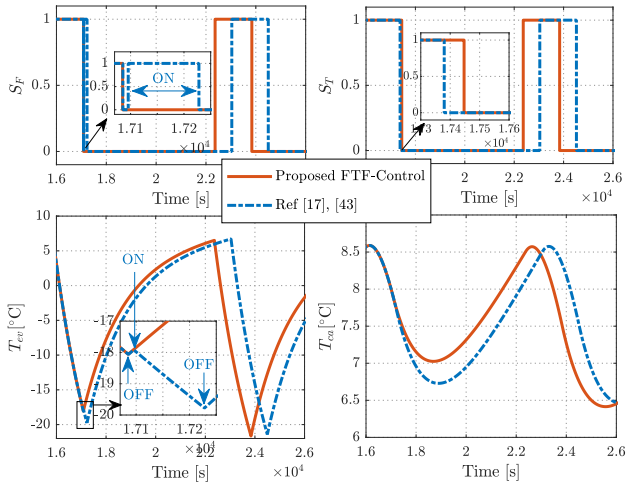

Fig. 16. Comparison to the existing strategy from [17], [43] for final status of switch S_F, conventional switch S_T, evaporator temperature T_{ev} [°C] and cavity temperature T_{ca} [°C].

V. CONCLUSION

This paper proposes an autonomous and decentralized FTF refrigerator controller to provide FFC service. It is observed that a refrigerator aggregation follows the prescribed frequency and temperature operating range that enables refrigerators to

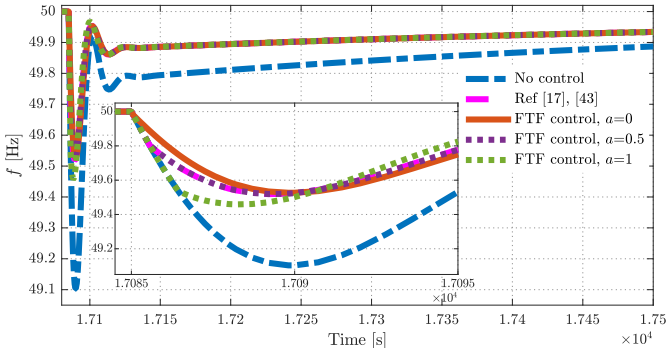

Fig. 17. Comparison of the system frequency f [Hz] with the strategy proposed in [17], [43] incorporating a communication delay.

dynamically modify their power usage in proportion to the frequency deviations and the cavity temperature. A rapid active power response from the refrigerators significantly improves the frequency security parameters, *i.e.* RoCoF and frequency nadir. Quick active power delivery by the refrigerators with reduced power consumption following the frequency threshold crossing is found similarly effective as conventional spinning reserve response and with shorter delivery time.

Further, it is observed that the thermodynamic performance of the refrigerators in terms of the cavity and evaporator temperature has a negligible effect on their normal operation. Simultaneous and abrupt switching to minimize bulk participation of refrigerators for FFC is well managed by the adaptive FTF controller autonomously, without compromising the users' comfort. The refrigerator participation in FFC can be increased by introducing certain modifications in the threshold and membership function of the frequency and temperature. The proposed work can be potentially enhanced by integrating diverse TCL devices, resulting in a more flexible overall performance.

REFERENCES

[1] L. Meng, J. Zafar, S. K. Khadem, A. Collinson, K. C. Murchie, F. Coffele, and G. M. Burt, "Fast frequency response from energy storage system—a review of grid standards, projects and technical issues," *IEEE Trans. on Smart Grid*, vol. 11, no. 2, pp. 1566–1581, 2020.

[2] V. Prakash and H. Pandzic, "Fast frequency control service provision from active neighborhoods: Opportunities and challenges," *Electric Power Syst. Res.*, vol. 217, p. 109161, 2023.

[3] V. Prakash, K. C. Sharma, R. Bhakar, H. P. Tiwari, and F. Li, "Frequency response constrained modified interval scheduling under wind uncertainty," *IEEE Trans. on Sust. Energy*, vol. 9, no. 1, pp. 302–310, 2018.

[4] V. Lakshmanan, M. Marinelli, J. Hu, and H. W. Bindner, "Provision of secondary frequency control via demand response activation on thermostatically controlled loads: Solutions and experiences from denmark," *Appl. Energy*, vol. 173, pp. 470–480, 2016.

[5] J. Yang, Z. Li, K. Ma, S. Liu, and S. Guo, "Energy priority control strategy and reward allocation mechanism for thermostatically controlled loads based on leaky storage model," *Electric Power Syst. Res.*, vol. 211, p. 108159, 2022.

[6] M. T. Muhssin, L. M. Cipcigan, S. S. Sami, and Z. A. Obaid, "Potential of demand side response aggregation for the stabilization of the grids frequency," *Appl. Energy*, vol. 220, pp. 643–656, 2018.

[7] F. Conte, M. Crosa di Vergagni, S. Massucco, F. Silvestro, E. Ciapessoni, and D. Cirio, "Performance analysis of frequency regulation services provided by aggregates of domestic thermostatically controlled loads," *Int. J. of Elect. Power & Energy Syst.*, vol. 131, p. 107050, 2021.

[8] C. Li, C. Feng, J. Li, D. Hu, and X. Zhu, "Comprehensive frequency regulation control strategy of thermal power generating unit and ess considering flexible load simultaneously participating in agc," *J. of Energy Storage*, vol. 58, p. 106394, 2023.

[9] J. Hu, J. Cao, M. Z. Q. Chen, J. Yu, J. Yao, S. Yang, and T. Yong, "Load following of multiple heterogeneous tcl aggregators by centralized control," *IEEE Trans. on Power Syst.*, vol. 32, no. 4, pp. 3157–3167, 2017.

[10] C. Gao, M. Song, S. Ma, M. Guo, R. Lv, and F. Fei, "Dynamic modelling and optimal control of virtual power plant driven by commercial hvacs," *IET Renewable Power Gener.*, vol. 16, no. 12, pp. 2590–2603, 2022.

[11] M. Bagheri-Sanjareh, M. H. Nazari, and S. H. Hosseinian, "Coordination of hybrid energy storage system, photovoltaic systems, smart lighting loads, and thermostatically controlled loads for microgrid frequency control," *Int. Trans. on Elec. Energy Sys.*, vol. 31, no. 8, p. e12976, 2021.

[12] B. Lundstrom, S. Patel, S. Attree, and M. V. Salapaka, "Fast primary frequency response using coordinated der and flexible loads: Framework and residential-scale demonstration," in *2018 IEEE Power & Energy Soc. General Meeting (PESGM)*. IEEE, 2018, pp. 1–5.

[13] C. Diaz-Londono, D. Enescu, F. Ruiz, and A. Mazza, "Experimental modeling and aggregation strategy for thermoelectric refrigeration units as flexible loads," *Appl. Energy*, vol. 272, p. 115065, 2020.

[14] N. Zhao, S. Gorbachev, D. Yue, V. Kuzin, C. Dou, X. Zhou, and J. Dai, "Model predictive based frequency control of power system incorporating air-conditioning loads with communication delay," *Int. J. of Elect. Power & Energy Syst.*, vol. 138, p. 107856, 2022.

[15] S. H. Tindemans, V. Trovato, and G. Strbac, "Decentralized control of thermostatic loads for flexible demand response," *IEEE Trans. on Control Syst. Technol.*, vol. 23, no. 5, pp. 1685–1700, 2015.

[16] S. Williams, M. Short, and T. Crosbie, "On the use of thermal inertia in building stock to leverage decentralised demand side frequency regulation services," *Appl. Thermal Eng.*, vol. 133, pp. 97–106, 2018.

[17] M. Cheng, J. Wu, S. J. Galsworthy, C. E. Ugalde-Loo, N. Gargov, W. W. Hung, and N. Jenkins, "Power system frequency response from the control of bitumen tanks," *IEEE Trans. on Power Syst.*, vol. 31, no. 3, pp. 1769–1778, 2016.

[18] M. Cheng, J. Wu, S. Galsworthy, N. Jenkins, and W. Hung, "Availability of load to provide frequency response in the great britain power system," in *2014 Power Syst. Computation Conf.* IEEE, 2014, pp. 1–7.

[19] V. Trovato, S. H. Tindemans, and G. Strbac, "Designing effective frequency response patterns for flexible thermostatic loads," in *2015 IEEE 15th Int. Conf. on Environ. and Elect. Eng. (EEEIC)*. IEEE, 2015, pp. 1003–1008.

[20] M. Eissa, A. Ali, K. Abdel-Latif, and A. Al-Kady, "A frequency control technique based on decision tree concept by managing thermostatically controllable loads at smart grids," *Int. J. of Elect. Power & Energy Syst.*, vol. 108, pp. 40–51, 2019.

[21] V. Trovato, I. M. Sanz, B. Chaudhuri, and G. Strbac, "Advanced control of thermostatic loads for rapid frequency response in great britain," *IEEE Trans. on Power Syst.*, vol. 32, no. 3, pp. 2106–2117, 2017.

[22] M. Aunedi, P.-A. Kountouriotis, J. O. Calderon, D. Angeli, and G. Strbac, "Economic and environmental benefits of dynamic demand in providing frequency regulation," *IEEE Trans. on Smart Grid*, vol. 4, no. 4, pp. 2036–2048, 2013.

[23] H. Zhao, Q. Wu, S. Huang, H. Zhang, Y. Liu, and Y. Xue, "Hierarchical control of thermostatically controlled loads for primary frequency support," *IEEE Trans. on Smart Grid*, vol. 9, no. 4, pp. 2986–2998, 2016.

[24] A. Kasis and I. Lestas, "Frequency regulation with thermostatically controlled loads: Aggregation of dynamics and synchronization," *IEEE Trans. on Autom. Control*, vol. 67, no. 10, pp. 5602–5609, 2022.

[25] J. A. Short, D. G. Infield, and L. L. Freris, "Stabilization of grid frequency through dynamic demand control," *IEEE Trans. on Power Syst.*, vol. 22, no. 3, pp. 1284–1293, 2007.

[26] Q. Shi, F. Li, G. Liu, D. Shi, Z. Yi, and Z. Wang, "Thermostatic load control for system frequency regulation considering daily demand profile and progressive recovery," *IEEE Trans. on Smart Grid*, vol. 10, no. 6, pp. 6259–6270, 2019.

[27] I. M. Alotaibi, M. Abido, and M. Khalid, "Primary frequency regulation by demand side response," *Arabian J. for Sci. and Eng.*, pp. 1–11, 2021.

[28] N. Farquhar and J. L. Mathieu, "Demand response potential of residential thermostatically controlled loads in michigan," in *2019 IEEE Power & Energy Soc. General Meeting (PESGM)*. IEEE, 2019, pp. 1–5.

[29] G. Liu, Y. Tao, L. Xu, Z. Chen, J. Qiu, and S. Lai, "Coordinated management of aggregated electric vehicles and thermostatically controlled

loads in hierarchical energy systems," *Int. J. of Elect. Power & Energy Syst.*, vol. 131, p. 107090, 2021.
[30] E. Vrettos, E. C. Kara, J. MacDonald, G. Andersson, and D. S. Callaway, "Experimental demonstration of frequency regulation by commercial buildings—part i: Modeling and hierarchical control design," *IEEE Trans. on Smart Grid*, vol. 9, no. 4, pp. 3213–3223, 2018.
[31] M. Song, W. Sun, Y. Wang, M. Shahidehpour, Z. Li, and C. Gao, "Hierarchical scheduling of aggregated tcl flexibility for transactive energy in power systems," *IEEE Trans. on Smart Grid*, vol. 11, no. 3, pp. 2452–2463, 2020.
[32] S. Bashash and H. K. Fathy, "Modeling and control of aggregate air conditioning loads for robust renewable power management," *IEEE Trans. on Control Sys. Tech.*, vol. 21, no. 4, pp. 1318–1327, 2013.
[33] J. L. Mathieu, S. Koch, and D. S. Callaway, "State estimation and control of electric loads to manage real-time energy imbalance," *IEEE Trans. on Power Sys.*, vol. 28, no. 1, pp. 430–440, 2013.
[34] ENTSO-E, Demand Connection Code (draft 21 December 2012).
[35] K.-Y. Cai and L. Zhang, "Fuzzy reasoning as a control problem," *IEEE Trans. on Fuzzy Syst.*, vol. 16, no. 3, pp. 600–614, 2008.
[36] Y. Lu, "Adaptive-fuzzy control compensation design for direct adaptive fuzzy control," *IEEE Trans. on Fuzzy Syst.*, vol. 26, no. 6, pp. 3222–3231, 2018.
[37] A. Abazari, H. Monsef, and B. Wu, "Coordination strategies of distributed energy resources including fess, deg, fc and wtg in load frequency control (lfc) scheme of hybrid isolated micro-grid," *In. J. of Elec. Power & Energy Syst.*, vol. 109, pp. 535–547, 2019.
[38] V. Gholamrezaie, M. G. Dozein, H. Monsef, and B. Wu, "An optimal frequency control method through a dynamic load frequency control (lfc) model incorporating wind farm," *IEEE Syst. J.*, vol. 12, no. 1, pp. 392–401, 2018.
[39] H. R. Chamorro, I. Riaño, R. Gerndt, I. Zelinka, F. Gonzalez-Longatt, and V. K. Sood, "Synthetic inertia control based on fuzzy adaptive differential evolution," *Int. J. of Elec. Power & Energy Syst.*, vol. 105, pp. 803–813, 2019.
[40] S. Nema, V. Prakash, and H. Pandžić, "Adaptive synthetic inertia control framework for distributed energy resources in low-inertia microgrid," *IEEE Access*, vol. 10, pp. 54 969–54 979, 2022.
[41] E. H. Mamdani, "Application of fuzzy algorithms for control of simple dynamic plant," in *Proc. of the institution of electrical engineers*, vol. 121, no. 12. IET, 1974, pp. 1585–1588.
[42] L. A. Zadeh, "Outline of a new approach to the analysis of complex syst. and decision processes," *IEEE Trans. on Syst., Man, and Cybern.*, vol. SMC-3, no. 1, pp. 28–44, 1973.
[43] M. Cheng, "Dynamic demand for frequency response services in the great britain power system," Ph.D. dissertation, Cardiff Univ., 2014.
[44] C. Spallarossa, Y. Pipelzadeh, B. Chaudhuri, and T. Green, "Assessment of disturbance propagation between ac grids through vsc hvdc links using reduced great britain model," in *10th IET Int. Conf. on AC and DC Power Transmiss. (ACDC 2012)*, 2012, pp. 1–6.
[45] F. Teng, Y. Mu, H. Jia, J. Wu, P. Zeng, and G. Strbac, "Challenges on primary frequency control and potential solution from evs in the future gb electricity system," *Appl. Energy*, vol. 194, pp. 353–362, 2017.
[46] W. Hung, G. Ray, and G. Stein, "Frequency changes during large disturbances WG," Nat. Grid plc, August 2013.
[47] Y. Bian, H. Wang, H. Wyman-Pain, C. Gu, and F. Li, "Frequency response in the gb power system from responsive chps," *Energy Procedia*, vol. 105, pp. 2302–2309, 2017, 8th Int. Conf. on Appl. Energy, ICAE2016, 8-11 October 2016, Beijing, China.
[48] National Grid plc, 'The Grid Code – Issue 5, Revision 9', National Grid Electricity Transmiss.plc, pp. 188, July 2014.
[49] L. Harrington, L. Aye, and B. Fuller, "Impact of room temperature on energy consumption of household refrigerators: Lessons from analysis of field and laboratory data," *Appl. Energy*, vol. 211, pp. 346–357, 2018.
[50] "National Grid. Mandatory Frequency Response. 2016."
[51] "National Grid. Frequency Risk and Control Report, April, 2022."

Sumit Nema (Student Member, IEEE) received the B.E. and M.E. degrees from the Rajiv Gandhi Proudyogiki Vishwavidyalaya, Bhopal, Madhya Pradesh, India. He is currently pursuing the Ph.D. degree from Banasthali Vidyapith, Tonk, Rajasthan, India. His research interests include power system ancillary services planning, operation, control, and economics of power, energy systems and thermostatically control loads.

Vivek Prakash (Senior Member, IEEE) is currently serving as an Assistant Professor in the School of Automation, Banasthali Vidyapith, Rajasthan, India. His academic journey includes completing postdoctoral research at the Faculty of Electrical Engineering and Computing (FER), University of Zagreb, Croatia in 2022, and obtaining a PhD in Electrical Engineering from Malaviya National Institute of Technology Jaipur, India in 2019. His research interests include operations, control, and economics of power and energy systems.

Hrvoje Pandžić (Senior Member, IEEE) received the M.E.E. and Ph.D. degrees from the Faculty of Electrical Engineering and Computing, University of Zagreb, Croatia, in 2007 and 2011, respectively. From 2012 to 2014, he was a Postdoctoral Researcher with the University of Washington, Seattle, WA, USA. He is currently working as a Full Professor with the Faculty of Electrical Engineering and Computing, University of Zagreb, and the Head of the Department of Energy and Power Systems. His research interests include planning, operation, control, and economics of power and energy systems. He has been an Editor of the IEEE Transactions on Power Systems, since 2019.